Invariant pattern recognition by use of wavelength multiplexing

Zeev Zalevsky, David Mendlovic, and Javier García

Rotation-invariant pattern recognition can be achieved with circular-harmonic decomposition. A common problem with such a filter is that, because it is only a single term out of the circular decomposition, it does not contain much of the reference object's energy. Thus, the obtained correlation selectivity is low. This problem is solved by use of wavelength multiplexing. First, different harmonic terms are encoded by different wavelengths, and then they all are added incoherently in the output correlation plane. This process leads to rotation-invariant pattern recognition with a higher discrimination ability.
© 1997 Optical Society of America

Key words: Correlators, invariant pattern recognition, harmonic decomposition, multichannel systems, wavelength multiplexing.

1. Introduction

Optical pattern recognition is commonly performed with a $4f$ correlator.[1] This setup uses a matched filter that provides the highest signal-to-noise ratio for a Gaussian white noise but is not invariant to any parameter except lateral shifts of the input object. Other invariant properties could be obtained by use of harmonic decompositions. In this method the reference object is decomposed into a set of orthogonal harmonic functions, and the filter source is chosen as a single expansion order. This approach achieves invariant pattern recognition, but its discrimination abilities are worse than those of the conventional matched-filter approach because here the filter is only a single term out of the full harmonic decomposition.

Suggested decompositions for obtaining invariant properties were circular-harmonics for rotation invariance,[2] radial harmonics (RH) for scale invariance,[3] and logarithmic harmonics (LH) for projection invariance.[4] Later, the harmonic-decomposition method was generalized for other distortion properties by use of deformation harmonics (DH).[5] These methods are optimized by the choice of the proper center for harmonic expansion and the proper harmonic order for the filter.[6,7]

Another method that permitted achieving both invariant pattern recognition and high discrimination ability is the synthetic-discriminant-function approach.[8] The problem with this method was that an invariant property was achieved only in the correlation peak itself, and it was commonly followed by unacceptable levels of sidelobes.

In this paper we propose a method that permits the achievement of full invariant pattern recognition while the filter combines several harmonic orders simultaneously. The method is demonstrated with circular harmonics, but any other decomposition set (RH, LH, DH) may be used. In this approach each harmonic order is transmitted with a different wavelength. At the output correlation plane all correlation distributions coming from the different decomposition orders are added incoherently. This finally provides improved discrimination ability.

In Section 2 we provide the necessary details regarding circular-harmonic (CH) decomposition. In Section 3 we explain and prove the suggested algorithm. In Section 4 we give an experimental demonstration.

2. Circular Harmonic Decomposition

CH decomposition is the first harmonic expansion that was used for invariant pattern recognition.[2] It involves the set of orthogonal functions $\{\exp(iN\theta)\}$,

Z. Zalevsky and D. Mendlovic are with the Faculty of Engineering, Tel-Aviv University, 69978 Tel-Aviv, Israel. J. García is with the Departament Interuniversitari d'Optíca, Facultat de Física, Universitat de València, Calle Doctor Moliner 50, 46100 Burjassot, Spain.

Received 4 March 1996; revised manuscript received 19 August 1996.
0003-6935/97/051059-05$10.00/0
© 1997 Optical Society of America

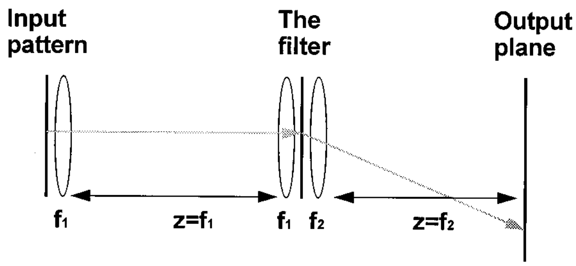

Fig. 1. Suggested optical setup for rotation-invariant pattern recognition.

which is multiplied by a radial function:

$$f(r, \theta) = \sum_{N=-\infty}^{\infty} f_N(r) \exp(iN\theta), \tag{1}$$

$$f_N(r) = \frac{1}{2\pi} \int_0^{2\pi} f(r, \theta) \exp(-iN\theta) \mathrm{d}\theta, \tag{2}$$

where N is the expansion order and $f(r, \theta)$ is the input object. A single-harmonic impulse response is thus $g(r, \theta) = f_M(r) \exp(iM\theta)$, and it can provide rotation-invariant pattern recognition by use of a single harmonic out of this expansion. The correlation between the target and a single-harmonic component at the origin of the correlation plane is given by

$$C_N = 2\pi \int_0^{\infty} |f_N(r)|^2 r \mathrm{d}r. \tag{3}$$

Correlation of the object with the same object rotated at an angle α, in terms of the correlation with different CH components, results in

$$C_\alpha = \sum_{N=-\infty}^{\infty} C_N \exp[iN\alpha]. \tag{4}$$

Equation (4) permits the interpretation of the rotation variance of a conventional matched filter. The correlation-peak contributions of the different CH components get out of phase except for $\alpha = 0$ (when $N \neq 0$). If only one CH is considered, the phase factor can be neglected when the output-plane intensity is taken. However, the simultaneous use of several harmonics may destroy the correlation peak as a result of differing phase factors. Multiple CH components can be used if the phase shift of each term in Eq. (4) is compensated.[9] This method, however, can be applied only to digital correlation or to the use of spatial multiplexing.[10]

3. Optical Implementation

The proposed method can be applied with different harmonic decompositions. We demonstrate it with the CH expansion used for rotation-invariant pattern recognition, but it can be extended to RH, LH, and DH. The optical setup for performing multiple-harmonic rotation-invariant pattern recognition by use of wavelength multiplexing is illustrated in Fig. 1. The input pattern should be illuminated by several spatially coherent wavelengths [for instance, a He–Ne laser (red), a doubled Nd:Yag laser (green), and an argon laser (blue)].

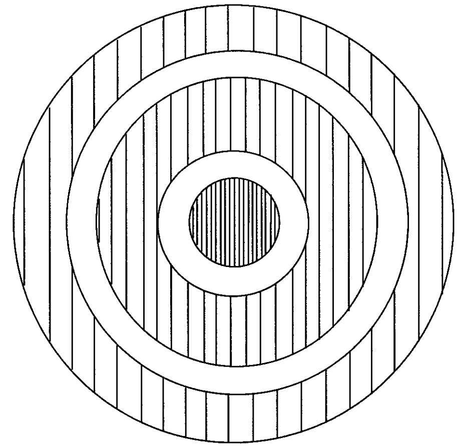
Fig. 2. Schematic sketch of the CH filter for three-wavelength multiplexing.

The first part of the setup performs a Fourier transform of the input pattern. A filter is placed in the Fourier plane and contains several rings, with each ring being a filter matched to a different order of the CH decomposition. The size of each ring is scaled with respect to the ratio between the different wavelengths used for the input illumination because an achromatic lens performs a Fourier transform that is scaled by λ_1/λ_i for the different wavelengths λ_i $\forall$ i. Each ring, which represents a different order of the CH decomposition, is applied to a different wavelength, i.e., each ring corresponds to a different wavelength. Thus, in the output plane the correlation peaks generated by the different harmonic orders are displayed in different wavelengths but at the same location and added in their intensities. Holograms with different spatial carrier frequencies are plotted inside each ring (each CH order). The ratio between the grating periods is as follows:

$$\sin \alpha = \frac{\lambda_i}{T_i} = \frac{\lambda_j}{T_j}, \tag{5}$$

where α is the angle of the first diffraction order from each grating, λ_i and λ_j are two different wavelengths, and T_i and T_j are the periods of the two corresponding gratings. Equation (5) ensures that different wavelengths λ_i and λ_j will diffract to the same spatial location. Because different wavelengths, coming from different rings (different CH orders), diffract to the same spatial position, they are added incoherently. A schematic illustration of the filter is given in Fig. 2.

The second part of the system performs another Fourier transform. Thus, in the output plane, an image of the input pattern is obtained after the pattern has passed through the CH filter. Each wavelength passes through a different CH order. If many wavelengths are used the output correlation plane is both rotation invariant and able to provide high discrimination comparable with that of the matched filter.

As mentioned above each harmonic order (each ring) is encoded by a different spatial frequency (see Fig. 2). Two contiguous rings should fulfill Eq. (5). This means that the first diffraction order coming from the grating that has the period T_1 and is illuminated by λ_1 and the first diffraction order coming from the grating that has the period T_2 and is illuminated by λ_2 should overlap. However, in addition we expect that the diffracted distributions coming from grating T_1 illuminated by λ_2 or from grating T_2 illuminated by λ_1 will not overlap with the desired distribution. Because the overall setup is an imaging setup with a magnification of f_2/f_1, one can translate the last restriction (nonoverlap) to the following mathematical condition:

$$f_2 \frac{\lambda_1/T_1}{\sqrt{1-({\lambda_1}^2/{T_1}^2)}} - f_2 \frac{\lambda_2/T_1}{\sqrt{1-({\lambda_2}^2/{T_1}^2)}} \geq 2L_x \frac{f_2}{f_1}, \quad (6)$$

where f_1 and f_2 are the focal lengths of the first and second parts of the setup, respectively, (see Fig. 1) and L_x is the size of the input image [the term $2L_x(f_2/f_1)$ is an approximation for the size of the correlation plane]. Using the approximation of $\sin\beta \approx \tan\beta$ permits Eq. (6) to be simplified to

$$T_1 \leq \frac{f_1(\Delta\lambda)}{2L_x}, \quad (7)$$

where $\Delta\lambda$ is the smallest difference between two wavelengths. Condition (7) gives us a restriction on the maximal value for the period of the gratings.

In this setup the ring sizes and CH components must be chosen to maximize the energy contents of the filter. A different approach can be used to utilize every CH component fully. We can accomplish this by multiplexing the filters for the different wavelengths. This multiplexing, although troublesome in computer-generated holograms (CGH's), is easy for optically recorded holograms (provided there is a small number of holograms). Thus, each CH filter should be recorded at the same angle for the reference beam but with the use, in each exposure, of a different wavelength. This approach will provide the same periods for the carrier frequencies as the above-described procedure. The final output intensity for a target rotated by an angle α, in the notation introduced in Section 2, is given by

$$I_\alpha = |C_\alpha|^2 = \sum_{N=-\infty}^{\infty} |C_N^\lambda|^2, \quad (8)$$

where the superscript λ gives the wavelength with which each correlation is obtained. The addition is obtained in the intensity, which is in contrast to the matched-filter case in which there is coherent addition. Nevertheless, now there is no variation with the rotation angle of the target, and every component contributes to the intensity of the correlation peak.

4. Chromatic Aberrations

The experimental problem raised when several wavelengths are used with achromatic lenses is chromatic aberration.[11,12] These aberrations are expressed as shifts of the focal length as a function of wavelength. This shift is caused by the dependence of the refraction index on the wavelength:

$$\frac{1}{F_{AL}(\lambda)} = \frac{n(\lambda)-1}{F_{AL}(\lambda_0)[n(\lambda_0)-1]}, \quad (9)$$

where $F_{AL}(\lambda_0)$ is the focal length of the achromatic lens for the wavelength of λ_0 and n is the refractive index. The dependence of the refractive index n on the wavelength may be approximated as

$$n(\lambda) \approx n(\lambda_0) - d(\lambda - \lambda_0), \quad (10)$$

where d is a constant.

If a zone plate is attached to the achromatic lens, the overall focal length becomes

$$\frac{1}{F(\lambda)} = \frac{1}{F_{ZP}(\lambda)} + \frac{1}{F_{AL}(\lambda)}, \quad (11)$$

where $F_{ZP}(\lambda)$ is the focal length of the zone plate, whose wavelength dependence may be expressed as

$$F_{ZP}(\lambda) = \frac{\lambda}{\lambda_0} F_{ZP}(\lambda_0). \quad (12)$$

Thus, by using Eqs. (9), (11), and (12) one obtains

$$\frac{1}{F(\lambda)} = \lambda\left\{\frac{1}{\lambda_0 F_{ZP}(\lambda_0)} - \frac{d}{[n(\lambda_0)-1]F_{AL}(\lambda_0)}\right\} + \frac{n(\lambda_0)+d\lambda_0-1}{F_{AL}(\lambda_0)[n(\lambda_0)-1]}. \quad (13)$$

The first term on the right-hand side is responsible for chromatic aberrations. Choosing

$$F_{ZP}(\lambda_0) = \frac{[n(\lambda_0)-1]F_{AL}(\lambda_0)}{\lambda_0 d} \quad (14)$$

ensures the elimination of those aberrations.

Keeping the deviation of the wavelength λ from the wavelength λ_0 small and choosing achromatic lenses made out of a material with a small d value ensure negligible aberrations. Note that, for the suggested wavelength-multiplexing approach, the difference between the various wavelengths does not have to be large. Small deviations will also ensure the desired spatial incoherence.

5. Experimental Results

To demonstrate the abilities of the new approach we have performed several experiments. The reference object is decomposed into the CH decomposition, and two orders are chosen out of this decomposition (according to energy and peak-sharpness considerations[7]). We chose orders 2 and 5. Obviously, when decomposition into circular harmonics occurs, the proper center (once again according to energy and peak-sharpness considerations[6]) is also chosen.

To improve performance we prepared a phase-only filter out of each circular harmonic. Because the filter is designed for two orders of circular harmonic, it should be illuminated by two wavelengths. We chose to work with the doubled Nd:Yag (532-nm) and He–Ne (632.8-nm) lasers. Each circular harmonic was modulated by a different carrier frequency (grating) such that conditions (6) and (7) are fulfilled. To encode the phase of the filter we used a CGH.[13] However, to do so we must first calculate the number of periods of the grating that enter into each pixel of the matrix (which contains the CH information) that we wish to encode. The minimal number of periods in each pixel of the matrix must be

$$n_0 = \frac{L_\nu/N}{T_1}, \tag{15}$$

where N is the number of pixels inside the matrix (in our case, $N = 128$) and L_ν is the size of the filter. Because the fast-Fourier-transform algorithm was used for the calculations, the following scaling ratio should be held between the sizes of the input plane and the spectral plane (see Ref. 14, for instance):

$$L_x L_\nu = \lambda f_1 N. \tag{16}$$

Substituting condition (7) and Eq. (16) into Eq. (15) yields

$$n_0 \geq \frac{2\lambda}{\lambda_1 - \lambda_2}. \tag{17}$$

Calculation with condition (17) leads to a value of $n_0 \geq 10.6$. We chose to use 12 periods per pixel. Next, using Lohmann's CGH method of vertical encoding, we create the filter. Each pixel of the filter contains 12 grating periods, encoded so that the compatible phase of the pixel of the matrix will be reconstructed.

Note that the final filter is composed of two matrices: The first one encodes the second CH order, and the second one encodes the fifth harmonic. The ratio between the gratings inside each CH is set according to Eq. (5). Therefore, the second harmonic will correspond to the green laser and the fifth to the red one.

Figure 3 illustrates the input pattern scene. The upper image is of a fault object, and the lower image is of the reference object, rotated by 90°. In Fig. 4 one can see the obtained experimental results. The center image depicts the obtained color output (green and red); this is the correlation peak for both the fifth and second CH's. On the righthand side one can see the correlation plane obtained for the second harmonic (green) and on the lefthand side the correlation obtained for the fifth harmonic (in red). Improved discrimination ability and stronger correlation peaks are obtained for the multiplexed correlation (central image), as compared with the single only-red or only-green channels.

Figure 5(a) illustrates a three-dimensional plot of the region of interest of Fig. 4, whereas Fig. 5(b) is a plot of the peaks' cross sections. One can see here, as well, the improved correlation peak obtained for the multiplexed correlation. Note that the experimental results obtained in this paper are only supposed to show that the method works. More results are required before evaluation of the performance of the method can be carried out with certainty.

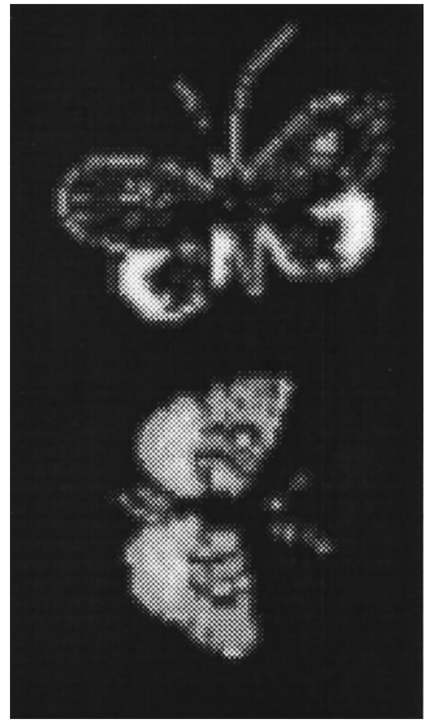

Fig. 3. Input scene used in the experiments.

6. Conclusion

From the experimental results one can see that the proposed filter provides improved discrimination ability and demonstrates a wide range of rotation invariance. Sharp correlation peaks were obtained. Note that the suggested technique was demonstrated for circular harmonics and achieved improved rotation-invariant pattern recognition. The same procedure may be applied to LH or RH. In this case, several orders of LH or RH are wavelength multiplexed (encoded in the different rings). In addition to achieving an improved single invariant property, one may obtain several invariant properties simultaneously. To do so, we choose one harmonic order out of several harmonic types (for example, CH and RH), and each harmonic type is multiplexed by a different

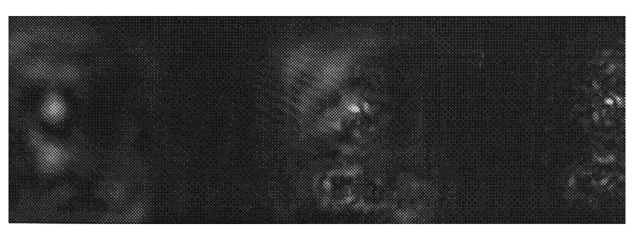

Fig. 4. Experimental output correlation plane.

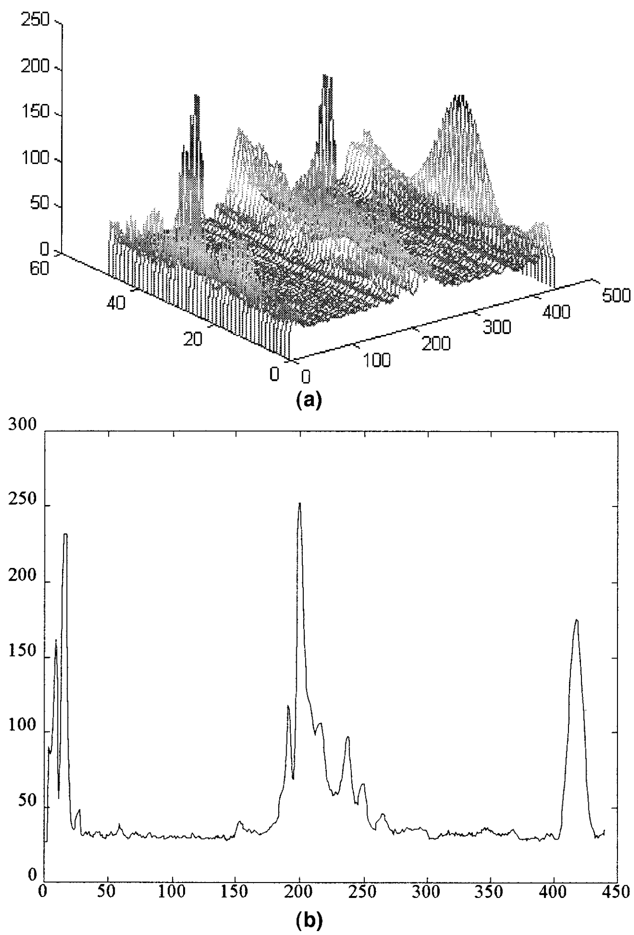

Fig. 5. (a) Three-dimensional plot of the obtained output correlation plane. (b) Plot of the peaks' cross section.

wavelength (i.e., each harmonic type is encoded in different ring of the filter). The result is correlation that is invariant to either rotation or scale.

Z. Zalevsky and D. Mendlovic acknowledge support provided by the Infrastructure Foundation and the Eshcol Foundation of the Israeli Ministry of Science and Technology.

References

1. A. VanderLugt, "Signal detection by complex spatial filtering," IEEE Trans. Inf. Theory **IT-10,** 139–145 (1964).
2. Y. N. Hsu and H. H. Arsenault, "Optical pattern recognition using the circular harmonic expansion," Appl. Opt. **21,** 4016–4019 (1982).
3. D. Mendlovic, E. Marom, and N. Konforti, "Shift and scale invariant pattern recognition using Mellin radial harmonics," Opt. Commun. **67,** 172 (1988).
4. D. Mendlovic, N. Konforti, and E. Marom, "Shift and projection invariant pattern recognition using logarithmic harmonics," Appl. Opt. **29,** 4784–4789 (1990).
5. E. Marom, D. Mendlovic, and N. Konforti, "Generalized spatial deformation harmonic filter for distortion invariant pattern recognition," Opt. Commun. **78,** 416–424 (1990).
6. P. García-Martinez, J. García, and C. Ferreira, "A new criterion for determining the expansion center for circular-harmonic filters," Opt. Commun. **117,** 399–405 (1995).
7. D. Mendlovic, Z. Zalevsky, J. García, and C. Ferreira, "Logarithmic harmonics proper expansion center and order for efficient projection invariant pattern recognition," Opt. Commun. **107,** 292–299 (1994).
8. D. Casasent and W. T. Chang, "Correlation synthetic discriminant functions," Appl. Opt. **25,** 2343 (1986).
9. Y. N. Hsu and H. H. Arsenault, "Pattern discrimination by multiple circular harmonic components," Appl. Opt. **23,** 841–844 (1984).
10. R. Wu and H. Stark, "Rotation invariant pattern recognition using vector reference," Appl. Opt. **23,** 838–840 (1984).
11. G. M. Morris, "Diffraction theory for an achromatic Fourier transformation," Appl. Opt. **20,** 2017–2025 (1981).
12. T. Stone and N. George, "Hybrid diffractive–refractive lenses and achromats," Appl. Opt. **27,** 2960–2971 (1988).
13. A. W. Lohmann and D. P. Paris, "Binary Fraunhofer holograms, generated by computer," Appl. Opt. **6,** 1739–1748 (1967).
14. J. García, R. G. Dorsch, and D. Mas, "Fractional Fourier transform calculation through fast Fourier transform algorithm," Appl. Opt. (to be published).